

An Application of Deep Learning Technology in The Recognition of Forged Documents with Color Laser Printing

Yung-Fou Chen¹, Hsin-Hsiung Kao², Chih-Ping Yen^{2*}

¹ Department of Forensic Science, Central Police University, Taoyuan 333322, Taiwan, ROC

² Department of Information Management, Central Police University, Taoyuan 333322, Taiwan, ROC

{nanoforensics, kao, peter}@mail.cpu.edu.tw

Received 19 August 2022; Revised 18 March 2023; Accepted 2 May 2023

Abstract. Advanced laser printing technology is now widely used in daily life and at work. Because laser printers are so easy to obtain and use, they have also become a popular method for criminals to forge important documents like currency, securities, and certificates. To obtain evidence for document forgery, traditional forensics use chemical analysis of ink, but the cost is high. Laser color printing uses halftone technology. This technology combines the CMYK printing colors' halftone screens at their respective angles. When correctly superimposed, they will form a moiré pattern. And the moiré pattern of a color block differs depending on the printer brand or model. This paper will use deep learning to create an image recognition model that can quickly classify forged documents by combining image processing, data augmentation, and transfer learning. The experimental results are examined using indicators of accuracy, precision, recall, F1-score, and PR curve. The results show that ResNet-50 has the best performance and can be used to detect document forgery. The study's findings will be useful for future criminal investigators and forensic personnel in their work.

Keywords: halftone technology, moiré pattern, deep learning, data augmentation, transfer learning

1 Introduction

The general method of identifying counterfeit documents, securities, and currency depends on the preset features of the document itself, and it is judged manually. For example, the NT dollar has the following preset features, including raised touch, watermark, color-changing ink, color-changing Security line, hidden characters, light and shadow change foil, metallic ink, light and shadow change of strip foil [1]. Today's advanced laser printing technology and low-cost printers make it easier to forge documents [2]. Recently, there have been many crimes of using counterfeit currency in many places in Taiwan [3]. Analytical techniques of toner powder, such as infrared spectroscopy (IR) [4], scanning electron microscope/energy dispersive X-ray analyzer (SEM/EDX) [5], pyrolysis gas chromatography-mass spectrometry (Py-GC-MS) [6], and Raman spectrometer [7], are commonly used for printing forensics [8]. However, the above methods are extremely expensive. In addition, the identification of counterfeit documents, securities, and currency is not the basic ability of criminal investigators. In order to make the investigation work smoothly, a simple identification method is studied, and then cloud technology is used to provide services, so that criminal investigators can quickly clarify the people, events, and objects in the case by using their smart phones.

Identification of counterfeit documents is often used to solve the problem of counterfeit banknotes. The methods of checking banknotes can be divided into three categories. Category 1 is manual visual inspection of banknote security features with microscope or ultraviolet (UV) radiation [9], which is intuitive and simple, but requires training and is also easily fooled by advanced counterfeiting techniques. The second category is to use chemical analysis to check the ink or toner. This method is reliable, but it requires complex analysis and interpretation, and the process is time-consuming and labor-intensive. The third category is to use image processing and pattern recognition. This method is also reliable, and has low cost and high efficiency. However, some research requires additional use of some imaging and scanning equipment. In addition, the recognition performance algorithm depends on the algorithm itself and number of training samples [10]. A number of methods have been proposed for the research of category 3 above. Gupta *et al.* [11] proposed to identify through the default printing characteristics of different printers. Sarkar *et al.* [12] took blue, green, red channels, and UV images, and then selects 7 features from them to classify with cascade of classifiers. Baek *et al.* [13] consider counterfeit banknote

* Corresponding Author

detection algorithms using IR images. Pachón *et al.* [14] used ultraviolet light (UV) to obtain the default security features of banknotes, and then confirmed that using ResNet18 for identification can obtain the best performance. Yeh *et al.* [15] used webcam to take banknote images, which were divided into multiple partitions and converted into brightness histograms, and then recognized based on multi-core support vector machines. Mohamad *et al.* [16] applied the method of artificial neural network and trained with backpropagation, but unfortunately there are no experimental results. Ali *et al.* [17] employed generative adversarial networks (GANs) for unsupervised learning to train a model, which is then used to perform supervised predictions. Jadhav *et al.* [18] manually extracted feature regions of banknotes, and then uses deep learning for identification. Laavanya *et al.* [19] combined AlexNet and transfer learning technology for counterfeit banknote identification. Krishna *et al.* [20] proposed convolutional neural networks (CNNs) to build an automatic fake currency recognition system (AFCRS), which can be deployed on smartphones, but this study lacks experimental results. Veeramsetty *et al.* [21] developed a novel lightweight convolutional neural network model for mobile device applications to recognize banknotes. Pham *et al.* [22] used smartphones to directly obtain banknote images, and extracted artificially designated ROI areas for identification. The experimental results proved that ResNet-18 had better average accuracy. Apoloni *et al.* [23] adopted a pure image processing method, including algorithms such as Canny edge detection, Hough line transform, optical character recognition and K-Means clustering.

Laser color printing uses halftone technology, which combines halftone screens of printed cyan, magenta, yellow, and black colors at their respective angles. When the angles are superimposed correctly, a moiré pattern known as a printing rosette is formed [24]. As shown in Fig. 1, the moiré pattern can become sufficiently noticeable to be visible in color.

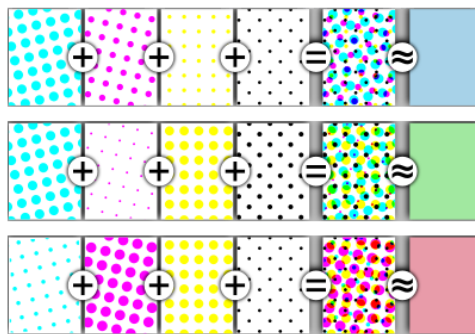
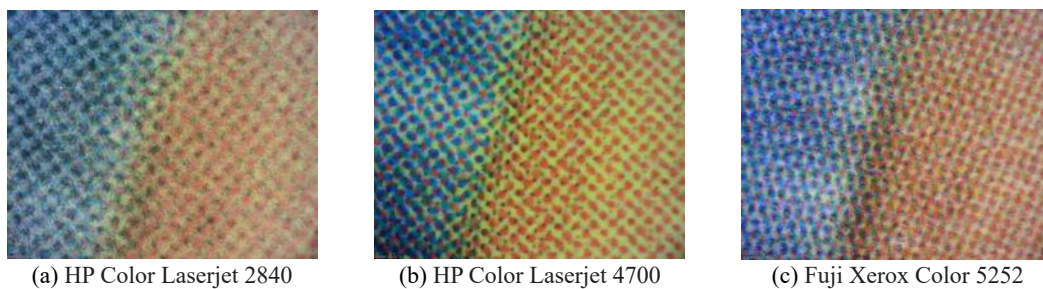


Fig. 1. Combined halftone pattern observed from sufficient distance [25]

For a moiré pattern of a color block, each brand or model of printer is different, as shown in Fig. 2. Therefore, based on deep learning technology, this research will construct a simple image recognition model for classifying moiré patterns of forged documents. For NT\$1000, Fig. 3(a) is the moiré pattern of the genuine banknote, while Fig. 3(b) is the moiré pattern of the counterfeit banknote.



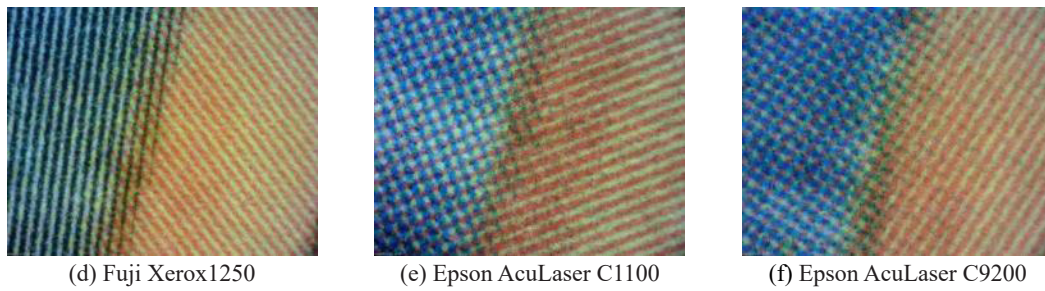


Fig. 2. Moiré pattern for a color block printed differently by different brands or models of printers [26]

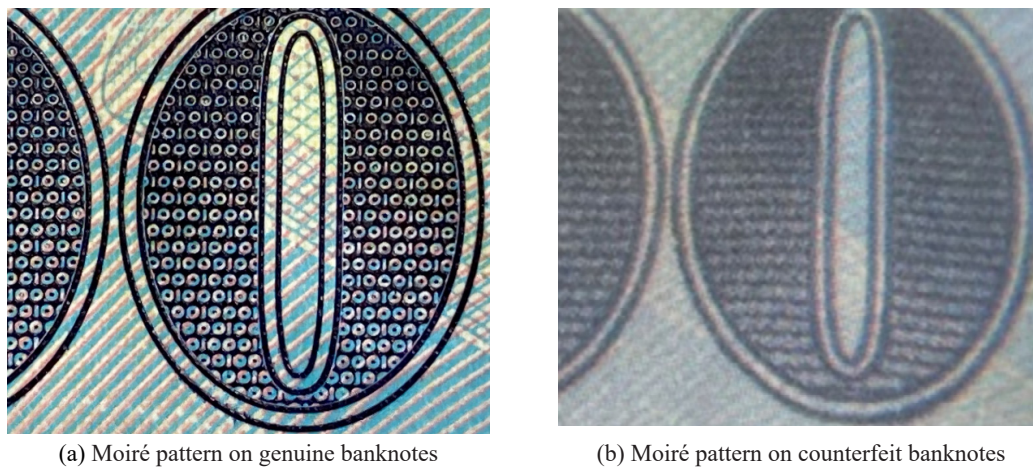


Fig. 3. A block of one thousand NT dollars

Since laser printing is a relatively easy and common means of counterfeiting documents, this paper proposes a simple and assisted identification method using Moiré pattern, and uses New Taiwan dollars as an example to prove the feasibility of the method. However, the printing methods of various documents are different, so the resulting patterns are also different, and the establishment of pattern databases for various documents is a follow-up work to be completed. The rest of this paper is organized as follows. In the next section, briefly introduces deep learning applied to classification and segmentation. Section 3 presents the proposed recognition model. Sections 4 show experimental results and discussion. Finally, Section 5 concludes the whole paper.

2 Deep Learning Applied to Classification and Segmentation

Deep learning technology is used in the field of computer vision for classification, detection, localization, and segmentation [27]. And related trainers have also emerged.

In classification technology, the experimental results of two gray-scale and regular texture datasets, KTH_TIPS and CURET, show that ResNet-50 performs better [28]. ResNet [29] was Microsoft's champion trainer in the 2015 ILSVRC competition [30], and its classification error rate is reduced to 3.5%, which is lower than the classification error rate of human eye recognition, which is 5%. Deepening the neural network's hidden layer usually improves performance, but the training results may be worse due to the vanishing gradient. Therefore, Res-Net employs residual connections to facilitate deeper network training and has developed various structural forms, including ResNet-18, ResNet-34, ResNet-50, ResNet-101, and ResNet-152. ResNet-50's architecture is divided into six sections: the first of which comprises $64 \times 7 \times 7$ convolution kernels and a 3×3 max pool. The second part is a block comprising several 1×1 , 3×3 , and 1×1 convolution kernels, with 9 layers after stacking three times. Similarly, the third part has 12 layers after stacking the block four times, the fourth part has 18 lay-

ers after stacking the block six times, and the fifth part has 9 layers after stacking the block three times. Average pooling, fully connected layer, and softmax make up the final output.

Table 1. Various structural forms of ResNet [29]

layer name	output size	18-layer	34-layer	50-layer	101-layer	152-layer
conv1	112×112	7×7, 64, stride 2				
		3×3 max pool, stride 2				
conv2_x	56×56	$\begin{bmatrix} 3 \times 3, 64 \\ 3 \times 3, 64 \end{bmatrix} \times 2$	$\begin{bmatrix} 3 \times 3, 64 \\ 3 \times 3, 64 \end{bmatrix} \times 3$	$\begin{bmatrix} 1 \times 1, 64 \\ 3 \times 3, 64 \\ 1 \times 1, 256 \end{bmatrix} \times 3$	$\begin{bmatrix} 1 \times 1, 64 \\ 3 \times 3, 64 \\ 1 \times 1, 256 \end{bmatrix} \times 3$	$\begin{bmatrix} 1 \times 1, 64 \\ 3 \times 3, 64 \\ 1 \times 1, 256 \end{bmatrix} \times 3$
conv3_x	28×28	$\begin{bmatrix} 3 \times 3, 128 \\ 3 \times 3, 128 \end{bmatrix} \times 2$	$\begin{bmatrix} 3 \times 3, 128 \\ 3 \times 3, 128 \end{bmatrix} \times 4$	$\begin{bmatrix} 1 \times 1, 128 \\ 3 \times 3, 128 \\ 1 \times 1, 512 \end{bmatrix} \times 4$	$\begin{bmatrix} 1 \times 1, 128 \\ 3 \times 3, 128 \\ 1 \times 1, 512 \end{bmatrix} \times 4$	$\begin{bmatrix} 1 \times 1, 128 \\ 3 \times 3, 128 \\ 1 \times 1, 512 \end{bmatrix} \times 8$
conv4_x	14×14	$\begin{bmatrix} 3 \times 3, 256 \\ 3 \times 3, 256 \end{bmatrix} \times 2$	$\begin{bmatrix} 3 \times 3, 256 \\ 3 \times 3, 256 \end{bmatrix} \times 6$	$\begin{bmatrix} 1 \times 1, 256 \\ 3 \times 3, 256 \\ 1 \times 1, 1024 \end{bmatrix} \times 6$	$\begin{bmatrix} 1 \times 1, 256 \\ 3 \times 3, 256 \\ 1 \times 1, 1024 \end{bmatrix} \times 23$	$\begin{bmatrix} 1 \times 1, 256 \\ 3 \times 3, 256 \\ 1 \times 1, 1024 \end{bmatrix} \times 36$
conv5_x	7×7	$\begin{bmatrix} 3 \times 3, 512 \\ 3 \times 3, 512 \end{bmatrix} \times 2$	$\begin{bmatrix} 3 \times 3, 512 \\ 3 \times 3, 512 \end{bmatrix} \times 3$	$\begin{bmatrix} 1 \times 1, 512 \\ 3 \times 3, 512 \\ 1 \times 1, 2048 \end{bmatrix} \times 3$	$\begin{bmatrix} 1 \times 1, 512 \\ 3 \times 3, 512 \\ 1 \times 1, 2048 \end{bmatrix} \times 3$	$\begin{bmatrix} 1 \times 1, 512 \\ 3 \times 3, 512 \\ 1 \times 1, 2048 \end{bmatrix} \times 3$
	1×1	average pool, 1000-d fc, softmax				
FLOPs		1.8×10 ⁹	3.6×10 ⁹	3.8×10 ⁹	7.6×10 ⁹	11.3×10 ⁹

In terms of segmentation technology, Olaf Ronneberger *et al.* [31] proposed U-Net in 2015 to make predictions using a small amount of data. As shown in Fig. 4, this network is made up of a contracting path (encoding part, left side) and an extensive path (decoding part, right side), and the overall structure is completely symmetrical and roughly U-shaped. It won the ISBI challenge for neural structure segmentation of electron microscope images [32], and U-Net has since become the standard for all image segmentation tasks.

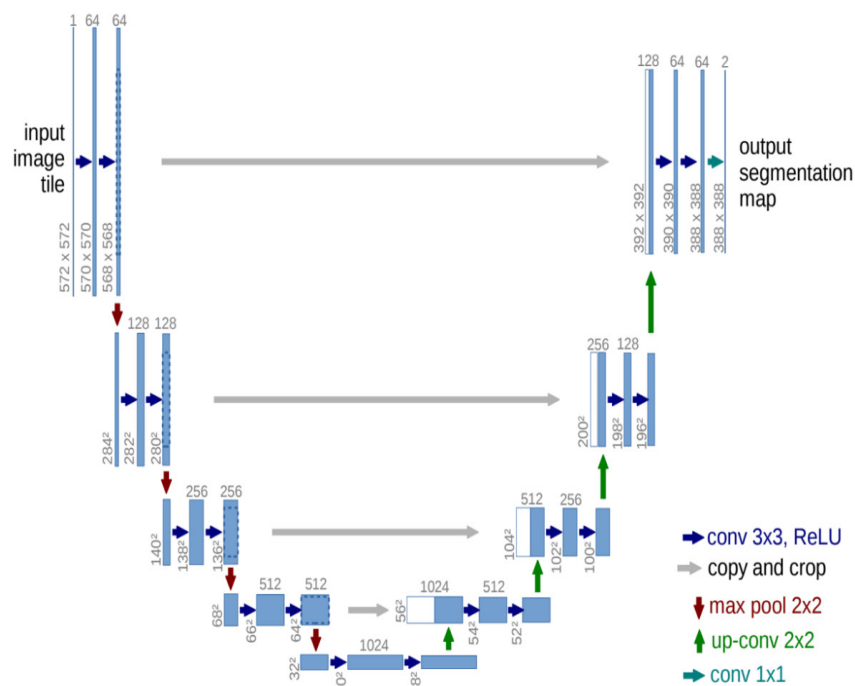


Fig. 4. Illustration of the U-net architecture [31]

U-Net is distinguished by its ability to combine and fuse high- and low-level features to generate feature maps of varying scales, thereby improving model accuracy. The U-Net architecture is divided into two parts: left and right decoders, each with a 4-layer down-sampling module and an up-sampling module; the two sides are linked by a skip connection. Furthermore, each blue block represents a multichannel feature map. The blue arrows indicate 3×3 convolution operations, and the activation functions are ReLU. The red arrows represent the 2×2 max pooling operation, which reduces the feature map size. Green arrows indicate 2×2 deconvolution operations. The gray arrows represent copy-and-cut operations used to fit the feature map on the left to the desired size on the right. The cyan arrow represents the output's final layer, which uses a 1×1 convolutional layer for classification.

3 Proposed Recognition Model

The purpose of this paper is document forgery recognition, so we first detect regions of interest (ROI) in documents based on deep learning to obtain ROI as a dataset. This dataset is further divided into training ROI and testing ROI, and then the training ROI performs data augmentation to obtain a sufficient number of experimental samples, and finally uses ResNet-50 and transfer learning technology to establish a recognition model, as shown in Fig. 5. The following subsections detail the important steps of the model.

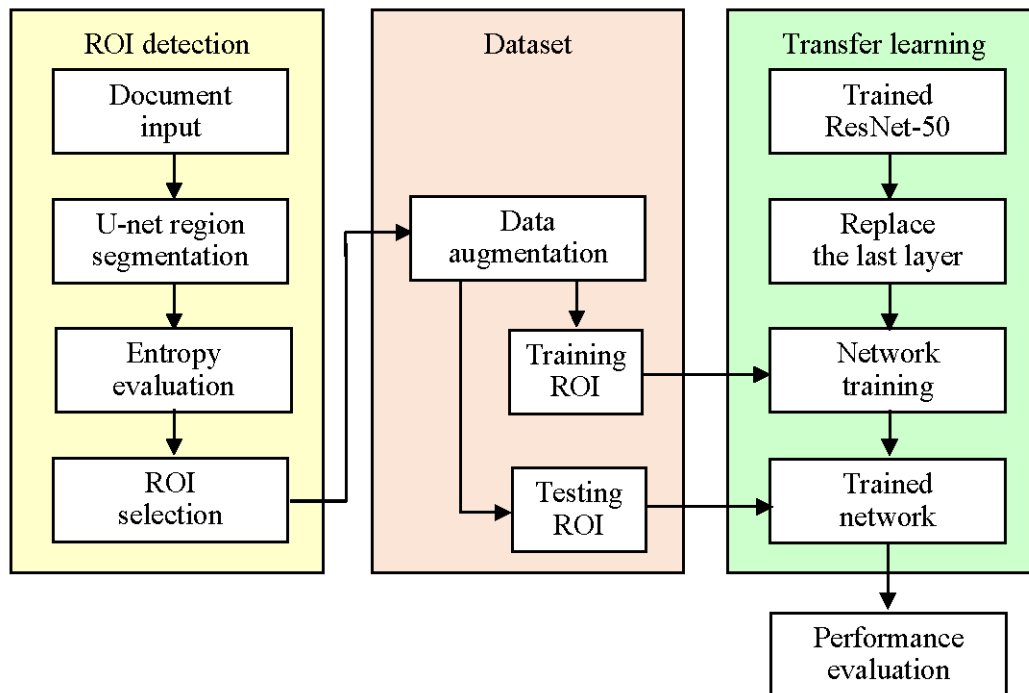


Fig. 5. Document forgery recognition model based on deep learning

3.1 ROI Detection

Document Input. High-resolution scanning of real and counterfeit paper documents to form electronic image files, this study will use New Taiwan dollar banknotes as an example.

U-net Region Segmentation. Use the trained U-net [33] to perform segmentation processing on the above electronic image files.

Entropy Evaluation. Information entropy was proposed by Shannon [34] to measure the degree of uncertainty in a system. That is to say, when the probability of an event happening is small, it means that there are fewer known parts, and there are more unknown parts hidden behind it, so more space should be reserved for description. In terms of image processing, formula (1) can be used to measure the information entropy of grayscale texture. A larger entropy value indicates that the brightness has a lot of texture detail changes, while a smaller entropy value indicates a flat texture with less detail changes [35].

$$E(I) = -\sum_{k=0}^{255} p(k) \log_2(p(k)), \tag{1}$$

where I is the original image, $E(I)$ is the information entropy value of the image I , and $p(k)$ is the probability that the grayscale value k appears in the image I . Fig. 6 shows some of the texture regions of the New Taiwan dollar banknote after the enlarged image, and the calculated information entropy value of these regions after converting to grayscale.

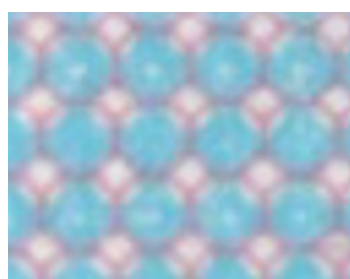


Fig. 6. The texture regions of the New Taiwan dollar banknote

ROI Selection. For each texture region of New Taiwan dollar banknotes, the one with the smallest information entropy value is selected as the data set. This is because under different paper materials, the moiré pattern is simpler and the individual differences are larger, which will be beneficial to the classification results to improve the performance.

3.2 Dataset

Data Augmentation. Since the collected dataset samples are limited, we use data augmentation to increase the number of samples [36]. This study employs 8 kinds of data augmentation, including horizontal flip, vertical flip, translation, rotation, scaling, brightness, blur, and shearing transformation. As described in Table 2, an additional 428 images will be obtained for each image.

Table 2. Data augmentation methods and descriptions

Method	Description	Number of obtained images
Horizontal flip	The ROI image is mirrored according to the center vertical line	1
Vertical flip	The ROI image is mirrored according to the center horizontal line	1
Translation	According to 1%, 2%, 3%, 4%, 5%, 6%, 7%, 8%, 9%, 10%, 11%, 12% of the image width and height, and to the surrounding 8 directions (up, down, left, right, upper left, lower left, upper right, lower right) displacement.	96
Rotation	Rotate clockwise and counterclockwise in increments of 2 until the angle is 90.	90
Scaling	Adjust the image using scaling factors such as 0.5, 0.55, 0.6, 0.65, 0.7, 0.75, 0.8, 0.85, 0.9, 0.95, 1.05, 1.1, 1.15, 1.2, 1.25, 1.3, 1.35, 1.4, 1.45, and 1.5.	20
Brightness	Adjust the brightness of the image, and increase the brightness to 30% in increments of 2%. Likewise, the 2% decrement darkens to 30%.	30
Blur	Blur with the following 2 filters: (i) Size 3x3 and 5x5 mean filters. (ii) Gaussian filter of size 3x3 and 5x5. And blur the image with standard deviation $\sigma = 0.1, 0.15, 0.2, 0.25, 0.3, 0.35, 0.4, 0.45, 0.5, 0.55$.	22
Shearing transformation	Shift each point horizontally or vertically by a proportional value, also known as the shear factor m . We perform horizontal and/or vertical shearing transformation of the image with $m = -0.6, -0.5, -0.4, -0.3, -0.2, -0.1, 0.1, 0.2, 0.3, 0.4, 0.5, 0.6$.	168

Training & Testing ROI. In order to augment the data, all the selected ROI images use data augmentation to form the experimental dataset, and this dataset is further divided into training ROI and testing ROI.

3.3 Transfer Learning

When the subject training data in a certain field is insufficient, or large-scale data collection and labeling are required at a high cost. In order to speed up the learning efficiency and avoid time-consuming retraining of all samples, transfer learning can be used to solve it [37]. The principle is that the more basic the pattern recognized by the front layer of the deep learning network, the more complex the pattern recognized by the later layer. For example, the first layer judges straight lines and very small circles, the second layer judges the combination and slightly complicated patterns of the previous layer, the third layer is more complicated, and so on. Since the features of the first few layers are common to all images, they can be retained, and as long as the latter layers are replaced, the newly added samples are then trained. According to the literature in Section 2, we know that the ResNet-50 deep learning model has good texture classification performance, so we use it to implement transfer learning. We delete the last prediction layer of the pre-trained ResNet-50 trainer, and then add a fully connected layer. Then train the aforementioned newly added Training ROI samples to achieve.

4 Experimental Results and Discussion

4.1 Experimental Environment

The experimental environment uses a personal computer with Intel Core i5-11400F CPU, 4.4GHz, 16G RAM and Windows 10 Pro (x64) operating system, and is executed in the Matlab R2020a development environment.

4.2 Moiré Pattern Dataset

We scan the banknotes with a resolution of 400 dpi, and obtain the ROI according to the U-net region segmentation and Entropy evaluation steps of the model in Fig. 5. Then, the banknotes were printed on six different laser printers and scanned with a resolution of 400 dpi to obtain individual moiré patterns, as shown in Fig. 7. The above six laser printers include RICOH SP C250, Epson AcuLaser C9200, HP Color LaserJet Enterprise M750, Fuji Xerox Color 5252, Canon MF644Cdw, Brother MFC-L8900CDW. The collected seven moiré patterns, that is, one is a real sample image, and the other six are fake sample images, all of which are augmented by horizontal flip, vertical flip, translation, rotation, scaling, brightness, blur, and shearing transformation. Since an additional 428 augmented images are obtained for each image, the dataset has a total of 3,003 moiré patterns. In addition, the experiment uses the hold-out method for validation, taking 50% of the samples for training about 1,505 images, and the remaining 50% for testing about 1,498 images.

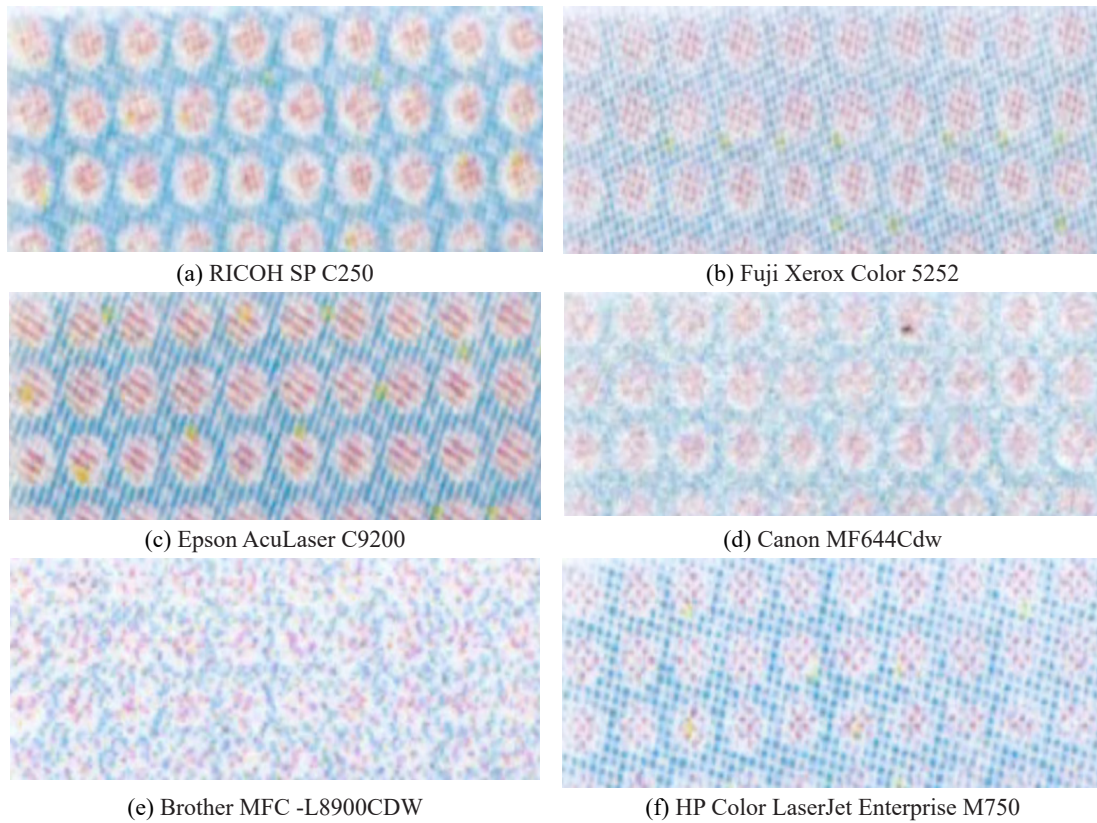


Fig. 7. Moiré patterns of ROI in banknotes using different laser printers including

4.3 Evaluation Indicators

The evaluation metrics used in this study include the first-level index confusion matrix, the second-level index accuracy, recall, and precision, the third-level index F1-score, and precision-recall curves [38]. The performance of the proposed document forgery recognition model is evaluated according to the above indicators, the formulas are as (2)-(5) respectively.

$$\text{Accuracy} = \frac{TP + TN}{TP + FP + TN + FN}, \quad (2)$$

$$\text{Precision} = \frac{TP}{TP + FP}, \quad (3)$$

$$\text{Recall} = \frac{TP}{TP + FN}, \quad (4)$$

$$\text{F1-score} = \frac{2 \times \text{Precision} \times \text{Recall}}{\text{Precision} + \text{Recall}}. \quad (5)$$

TP represents the number of correct predictions of the model as true for positive samples. Similarly, TN is the number of correctly predicted false positives for negative samples. FP shows the number of mispredictions of the model as true for negative samples, i.e. Type I error, or false alarm. Similarly, FN shows the number of mispredictions of the model as false for negative samples, i.e. Type II error, or missing alarm.

4.4 Experimental Results and Discussion

In addition to using ResNet-50 for recognition in this study, we also compare ResNet-18, ResNet-101 with different depths, and other commonly used and new deep learning trainers including AlexNet [39], VGGNet16 [40], VGGNet19 [40], GoogLeNet [41], Inception-v3 [42], Xception [43], DenseNet201 [44], MobileNetV2 [45]. The experimental results show that ResNet-50 has the best performance. Fig. 8 shows the confusion matrix of the recognition results of ResNet-50. Table 3 lists the performance comparisons of various trainers in detail. The relevant conclusions are as follows:

(i) The ResNet-50 model has the best recognition performance, with an accuracy of 98.87%, a precision of 94.98%, and a recall of 97.20%. The overall performance F1-score of 96.07% is also the best. From the above results, it shows that the ResNet-50 trainer is suitable for the recognition task of banknote texture.

(ii) It is found in Table 3 that the number of layers (depth) of the trainer affects the performance of the model, with deeper trainers representing better nonlinear processing capabilities.

(iii) The recognition performance of the ResNet-50 model is better than that of ResNet-18, which means that a deeper neural network can improve the performance. However, the depth of the neural network of ResNet-101 is deeper than that of ResNet-50, but it may be overfitting and the performance will be reduced. Therefore, the appropriate depth has the best performance.

True Class	Real	208	6	97.2%	2.8%
	Forgery	11	1273	99.1%	0.9%
		95.0%	99.5%	5.0%	0.5%
		Real	Forgery	Predicted Class	

Fig. 8. Confusion matrix of recognition results using ResNet-50

Table 3. Comparison of the performance of the proposed document forgery recognition models

Trainers	Layers	Evaluation indicator (%)			
		Accuracy	Precision	Recall	F1-Score
AlexNet	8	94.93	81.65	83.18	82.41
VGGNet16	16	95.26	82.35	85.05	83.68
VGGNet19	19	95.53	83.26	85.98	84.60
GoogLeNet	22	98.33	92.76	95.79	94.25
ResNet-18	18	97.93	91.40	94.39	92.87
ResNet-50	50	98.87	94.98	97.20	96.07
ResNet-101	101	98.46	93.61	95.79	94.69
Inception-v3	48	98.40	93.18	95.79	94.47
Xception	71	98.46	94.01	95.33	94.66
DenseNet201	201	98.33	93.55	94.86	94.20
MobileNetV2	28	97.73	91.67	92.52	92.09

Table 4 compares the effectiveness of our study with other 9 studies. These researches all directly use photographic technology to capture images without additional special equipment (such as UV, IR photography equipment). The comparison results show that our proposed method is better.

Table 4. Comparison of the performance of the proposed method and others

Method	Average accuracy
Yeh [15]	94.93
Mohamad [16]	N/A
Ali [17]	79.54%
Jadhav [18]	96.60%
Laavanya [19]	87.00%
Krishna [20]	N/A
Veeramsetty [21]	97.90%
Pham [22]	96.76%
Apoloni [23]	95.86%
Proposed	98.87%

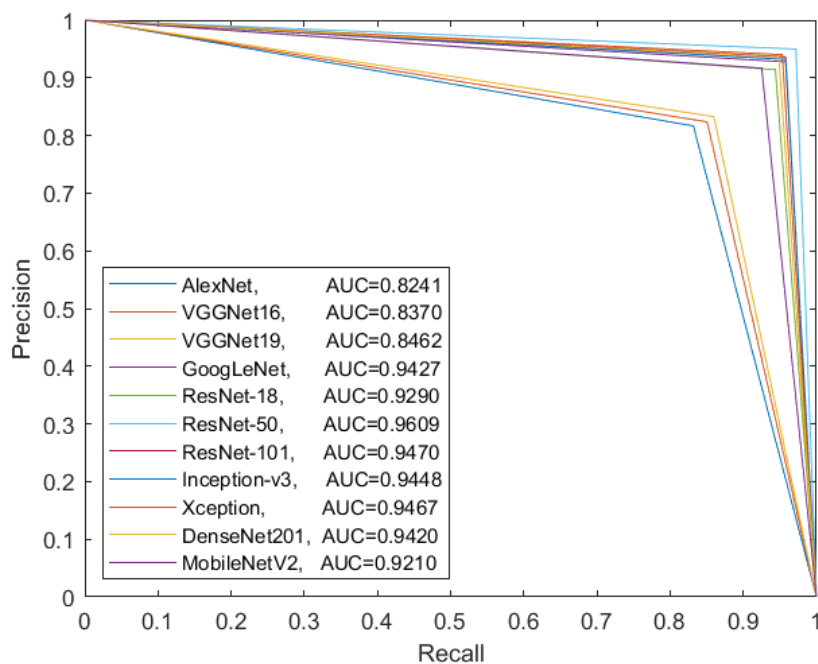


Fig. 9. PR curves and AUC values for various trainers

Fig. 9 is the PR curve, which represents the comprehensive performance of various trainers. The X-axis is recall, and the Y-axis is precision. The larger the area under the curve (AUC), the better the overall performance of precision and recall. Among them, the AUC value of ResNet-50 is the largest at 0.9609, followed by the AUC values of GoogLeNet, ResNet-101, Inception-v3, Xception, and DenseNet201, all reaching above 0.94. The difference between the first two AUC values is less than 3%, showing that these trainers are indistinguishable, and the AUC value of AlexNet is the smallest at 0.8241.

5 Conclusion

Color laser printers have become a popular tool for counterfeiting currency, securities, and certificates because they are relatively easy to obtain and use. Laser color printing uses halftone technology, which produces moiré patterns on the same block of colors that vary from brand to brand. In cases of forged documents, a quick and simple recognition method is required during the criminal investigation stage to help clarify the investigation's direction. Therefore, this study proposes a deep learning-based solution to the problem of expensive recognition caused by traditional chemical analysis. The main contribution of this study is to propose a simple method for identifying counterfeit documents, and to test it with the enlarged image of New Taiwan dollar banknotes captured by a smart phone as an example. Then it is suggested to use cloud technology to provide services, so that criminal investigators can use their smart phones to quickly clarify the people, events, and objects in the case. The results show that ResNet-50 performs better and is suitable for document counterfeiting detection. It has accuracy, precision, recall, an overall performance F1-score, and an AUC value of 98.87%, 94.98%, 97.20%, 96.07%, and 0.9609, respectively. In the future, our research will be directed toward more practical applications. We believe that using mobile phones with ultra-wide-angle macro lenses in conjunction with augmented reality (AR) technology will allow this study's recognition model to be implemented by an APP to assist criminal investigators and forensic personnel in the real-time investigation of forged documents.

Acknowledgments

This research was partially supported by the Science and Technology Projects of the Ministry of Interior (Improving the Quality of Forensic Science in Response to Judicial Reforms Project-112-0805-02-28-01).

References

- [1] New Taiwan Dollar Notes - Security Features, Central Engraving and Printing Plant. <<https://www.cepp.gov.tw/EN/Page?key=00cci>>, 2023 (accessed 20.01.23).
- [2] P. White, *Crime Scene to Court: The Essentials of Forensic Science*, 4th ed., Royal Society of Chemistry, 2016.
- [3] Y.J. Chiang, H.K. Hung, E. Kao, Counterfeit NT\$1,000 bills numbered HR484268XD seized across Taiwan, Focus Taiwan CNA English News. <<https://focustaiwan.tw/society/202301110009>>, 2023 (accessed 11.01.23).
- [4] J. Yu, J. Mao, T. Pan, P. Chen, L. Yao, Application of portable near-infrared spectrometer for analysis of organic carbon in marine sediments, *J. Geoscience Environ. Protection* 5(2017) 108-114.
- [5] Y.-F. Wang, B. Li, Determination of the sequence of intersecting lines from laser toner and seal ink by Fourier transform infrared microspectroscopy and scanning electron microscope/energy dispersive X-ray mapping, *Science & Justice* 52(2)(2012) 112-118.
- [6] E.J. Levy, T.P. Wampler, Applications of pyrolysis gas chromatography/mass spectrometry to toner materials from photocopiers, *Journal of Forensic Sciences* 31(1986) 258-271.
- [7] M.S. Božičević, A. Gajović, I. Zjakić, Identifying a common origin of toner printed counterfeit banknotes by micro-Raman spectroscopy, *Forensic Science International* 223(1-3)(2012) 314-320.
- [8] A. Tomar, R.R. Gupta, S.K. Mehta, S. Sachar, S. Sharma, A chronological overview of analytical techniques in forensic identification of printing toners, *TrAC Trends in Analytical Chemistry* 144(2021) 116450.
- [9] R.M. Correia, E. Domingos, F. Tosato, L.F.M. Aquino, A.M. Fontes, V.M. Cáo, P.R. Filgueiras, W. Romão, Banknote analysis by portable near infrared spectroscopy, *Forensic Chemistry* 8(2018) 57-63.
- [10] L. Wang, Y. Zhang, L. Xie, Z. Xiao, X. Guang, Z. Li, G. Shi, X. Hu, N. Zhang, Automated detection and classification of counterfeit banknotes using quantitative features captured by spectral-domain optical coherence tomography, *Science & Justice* 62(5)(2022) 624-631.

- [11] G. Gupta, S.K. Saha, S. Chakraborty, Document frauds: identification and linking fake document to scanners and printers, in: Proc. 2007 International Conference on Computing: Theory and Applications (ICCTA'07), 2007.
- [12] A. Sarkar, R. Verma, G. Gupta, Detecting counterfeit currency and identifying its source, in: Proc. IFIP International Conference on Digital Forensics, 2013.
- [13] S. Baek, E. Choi, Y. Baek, C. Lee, Detection of counterfeit banknotes using multispectral images, *Digital Signal Processing* 78(2018) 294-304.
- [14] C.G. Pachón, D.M. Ballesteros, D. Renza, Fake banknote recognition using deep learning, *Applied Sciences* 11(3) (2021) 12-81.
- [15] C.Y. Yeh, W.P. Su, S.J. Lee, Employing multiple-kernel support vector machines for counterfeit banknote recognition, *Applied Soft Computing* 11(1)(2011) 1439-1447.
- [16] N.S. Mohamad, B. Hussin, A.S. Shibghatullah, Banknote authentication using artificial neural network, in: Proc. International Symposium on Research in Innovation and Sustainability, 2014.
- [17] T. Ali, S. Jan, A. Alkhodre, M. Nauman, M. Amin, M.S. Siddiqui, DeepMoney: counterfeit money detection using generative adversarial networks, *PeerJ Computer Science* 5(2019) e216.
- [18] M. Jadhav, Y.K. Sharma, G.M. Bhandari, Currency identification and forged banknote detection using deep learning, International Conference on Innovative Trends and Advances in Engineering and Technology (ICITAET), 2019.
- [19] M. Laavanya, V. Vijayaraghavan, Real time fake currency note detection using deep learning, in: Proc. International Journal of Engineering and Advanced Technology 9(1S5)(2019) 95-98.
- [20] G.N. Krishna, G.S. Pooja, B.N.S. Ram, V.Y. Radha, P. Rajarajeswari, Recognition of fake currency note using convolutional neural networks, *International Journal of Innovative Technology and Exploring Engineering* 8(5)(2019) 58-63.
- [21] V. Veeramsetty, G. Singal, T. Badal, Coinnet: platform independent application to recognize Indian currency notes using deep learning techniques, *Multimedia Tools and Applications* 79(2020) 22569-22594.
- [22] T.D. Pham, C. Park, D.T. Nguyen, G. Batchuluun, K.R. Park, Deep learning-based fake-banknote detection for the visually impaired people using visible-light images captured by smartphone cameras, *IEEE Access* 8(2020) 63144-63161.
- [23] J.M.R. Apoloni, S.D.G. Escueta, J.T. Sese, Philippine currency counterfeit detector using image processing, in: Proc. 2022 IEEE 18th International Colloquium on Signal Processing & Applications (CSPA), 2022.
- [24] H.R. Kang, *Digital Color Halftoning*, SPIE, 1999.
- [25] Halftone, Wikipedia website. <<http://en.wikipedia.org/wiki/Halftone>>, 2022 (accessed 06.07.22).
- [26] Z.H. Lian, Color laser print identification, Published Master's Thesis, Central Police University, Taoyuan, Taiwan, 2009.
- [27] L. Alzubaidi, J. Zhang, A.J. Humaidi, A. Al-Dujaili, Y. Duan, O. Al-Shamma, J. Santamaría, M.A. Fadhel, M. Al-Amidie, L. Farhan, Review of deep learning: concepts, CNN architectures, challenges, applications, future directions, *Journal of Big Data* 8(1)(2021) 53.
- [28] P. Simon, U. V, Deep learning based feature extraction for texture classification, *Procedia Computer Science* 171(2020) 1680-1687.
- [29] K. He, X. Zhang, S. Ren, J. Sun, Deep residual learning for image recognition, in: Proc. 2016 IEEE Conference on Computer Vision and Pattern Recognition (CVPR), 2016.
- [30] ImageNet Large Scale Visual Recognition Challenge (ILSVRC). <<http://image-net.org/challenges/LSVRC/>>, 2010 (accessed 16.06.22).
- [31] O. Ronneberger, P. Fischer, T. Brox, U-Net: Convolutional networks for biomedical image segmentation, *Medical Image Computing and Computer-Assisted Intervention* (2015) 234-241.
- [32] UNI Freiburg. <<https://lmb.informatik.uni-freiburg.de/people/ronneber/isbi2015/>>, 2015 (accessed 06.07.22).
- [33] C. Karabağ, J. Verhoeven, N.R. Miller, C.C. Reyes-Aldasoro, Texture segmentation: an objective comparison between five traditional algorithms and a deep-learning U-Net architecture, *Applied Sciences* 9(18)(2019) 3900.
- [34] C.E. Shannon, A mathematical theory of communication, *The Bell System Technical Journal* 27(1948) 379-423.
- [35] R.C. Gonzalez, R.E. Woods, S.L. Eddins, *Digital Image Processing Using MATLAB*, 3rd ed., Gatesmark, 2020.
- [36] C. Shorten, T.M. Khoshgoftaar, A survey on image data augmentation for deep learning, *Journal of Big Data* 6(1)(2019) 60.
- [37] S.J. Pan, Q. Yang, A survey on transfer learning, *IEEE Transactions on Knowledge and Data Engineering* 22(10)(2010) 1345-1359.
- [38] E.R. Davies, *Computer Vision: Principles Algorithms Applications Learning*, 5th ed., Academic Press, 2017.
- [39] A. Krizhevsky, I. Sutskever, G. Hinton, ImageNet classification with deep convolutional neural networks, in: Proc. Advances in Neural Information Processing Systems, 2012.
- [40] K. Simonyan, A. Zisserman, Very deep convolutional networks for large-scale image recognition, in: Proc. 2015 International Conference on Learning Representations (ICRL), 2015.
- [41] C. Szegedy, W. Liu, Y. Jia, P. Sermanet, S. Reed, D. Anguelov, D. Erhan, V. Vanhoucke; A. Rabinovich, Going Deeper with Convolutions, in: Proc. 2015 IEEE Conference on Computer Vision and Pattern Recognition (CVPR), 2015.
- [42] C. Szegedy, V. Vanhoucke, S. Ioffe, J. Shlens, Z. Wojna, Rethinking the inception architecture for computer vision, in: Proc. 2016 IEEE Conference on Computer Vision and Pattern Recognition (CVPR), 2016.
- [43] F. Chollet, Xception: Deep learning with depthwise separable convolutions, in: Proc. 2017 IEEE Conference on Computer Vision and Pattern Recognition (CVPR), 2017.

- [44] G. Huang, Z. Liu, L.V.D. Maaten, K. Weinberger, Densely connected convolutional networks, in: Proc. 2017 IEEE Conference on Computer Vision and Pattern Recognition (CVPR), 2017.
- [45] M. Sandler, A. Howard, M. Zhu, A. Zhmoginov, L.C. Chen, MobileNetV2: Inverted residuals and linear bottlenecks, in: Proc. 2017 IEEE Conference on Computer Vision and Pattern Recognition (CVPR), 2018.